Visualization of the Optic Fissure in Short-Wavelength Autofluorescence Images of the Fundus

Tobias Duncker,[1] *Jonathan P. Greenberg,*[1] *Janet R. Sparrow,*[1] *R. Theodore Smith,*[1] *Harry A. Quigley,*[2] *and François C. Delori*[3]

Purpose. To document and explain the presence, inferior to the optic disc, of a distinct vertical boundary between two retinal areas of different short-wavelength autofluorescence (SW-AF) intensities.

Methods. SW-AF images of the inferonasal region were acquired from 32 healthy subjects. Additionally, color, 488-nm reflectance (488-R), near-infrared reflectance (NIR-R), NIR autofluorescence (NIR-AF) images, and a spectral domain optical coherence tomography (SD-OCT) image were obtained in selected subjects. Gray levels (GL) on both sides of the demarcation line were measured in SW-AF and 488-R at fixed distances from the disc center.

Results. A curved demarcation line inferior to the optic disc was observed on SW-AF images in 31/32 subjects. AF levels on the nasal side were 13% (±6%) lower than on the temporal side at 20° inferior to the disc center. The contrast between the nasal and the temporal areas was not significantly affected by age, sex, refractive error, race, or iris color. The demarcation line visible in SW-AF was also seen, though with reduced contrast, in approximately 80% of the 488-R images (lower reflectance on the nasal side) and 50% of color images. The boundary was not detected by NIR-R, NIR-AF, or by SD-OCT imaging.

Conclusions. The location and the distinctness of the demarcation line may indicate a relationship to the closed embryonic optic fissure. The reduced SW-AF intensity and 488-R reflectance observed on the nasal side of this line may be attributable to lower lipofuscin and melanin content per unit area, possibly resulting from a difference in RPE cell shape. (*Invest Ophthalmol Vis Sci.* 2012;53:6682–6686) DOI: 10.1167/iovs.12-10004

From the [1]Department of Ophthalmology, Harkness Eye Institute, Columbia University, New York, New York; the [2]Department of Ophthalmology, Wilmer Institute, Johns Hopkins University, Baltimore, Maryland; and the [3]Schepens Eye Research Institute and Department of Ophthalmology, Harvard Medical School, Boston, Massachusetts.

Supported by NEI R24 EY019861, NEI R01 EY015520, Foundation Fighting Blindness, NYC Community Trust, Roger H. Johnson Fund (University of Washington, Seattle), and a grant from Research to Prevent Blindness to the Department of Ophthalmology, Columbia University.

Submitted for publication April 10, 2012; revised July 16, 2012; accepted August 28, 2012.

Disclosure: **T. Duncker**, None; **J.P. Greenberg**, None; **J.R. Sparrow**, None; **R.T. Smith**, None; **H.A. Quigley**, None; **F.C. Delori**, None

Corresponding author: François C. Delori, Schepens Eye Research Institute, 20 Staniford Street, Boston, MA 02114; francois_delori@meei.harvard.edu.

Fundus autofluorescence (AF) imaging with blue light excitation (SW-AF) mainly reflects the distribution of RPE lipofuscin.[1] In retinal disorders, AF patterns have proven to be helpful diagnostic tools and a way to monitor disease progression. The wide clinical use of this imaging technique and recent efforts to quantify AF levels in subjects[2] reinforce the importance of identifying all factors that may influence the AF signal across the posterior pole.

Fundus SW-AF images often exhibit inferior to the optic disc a near-vertical discontinuity in the AF intensity, with lower AF on the nasal side. This demarcation line is visible in published high-quality SW-AF images recorded with a modified fundus camera,[3] scanning laser ophthalmoscope (SLO),[2,4–6] or with wide-field SLO.[7–9] However, to the best of our knowledge, this feature has never been described nor explained. Here, we investigated whether this feature can be seen in other imaging modalities and characterized the spatial and AF characteristics of this feature. We propose that this demarcation line indicates the location of the embryonic optic fissure.

Methods

The study population was 32 healthy subjects (18 females, 14 males) with a mean age of 32 years (range: 13–53 years) and normal eyes except for refractive error (ranging between −9 and +1 diopters), including 10 whites with blue or green iris color, 10 whites with brown or hazel iris color, 8 blacks, 3 Indians, and 1 Asian. An initial group of 12 subjects were selected for imaging of one (10) or both (2) eyes on the basis of the visibility of the demarcation line in standard AF images (fovea in the center of the field) obtained for a previous study.[2] The other 20 subjects were enrolled without prior knowledge of the fundus details and one (5) or both (15) eyes were imaged.

SW-AF images (30°) of the region inferior to the optic disc were acquired in all subjects in the high-speed mode with the Spectralis scanning laser ophthalmoscope (Heidelberg Engineering, Heidelberg, Germany) after pupil dilation with topical 1% tropicamide and 2.5% phenylephrine. Photopigments were bleached for 20 seconds[2] before image acquisition, and no histogram stretching was used in the processing of the image.

For the 12 subjects in the initial group, we also obtained color images with a FF450+IR fundus camera (Carl Zeiss Meditec, Jena, Germany), 55° AF, 488-nm reflectance (488-R), and near-infrared reflectance (NIR-R) images with the Spectralis-SLO, and near-infrared autofluorescence (NIR-AF) images with the HRA2-SLO (Heidelberg Engineering). Finally, a horizontal 9-mm SD-OCT scan of the same region was acquired with the Spectralis-SLO. All images were registered to each other with MatLab software (MathWorks, Natick, MA). Three observers independently assessed whether a boundary was visible in these images by side-by-side comparison with the SW-AF image. Interobserver agreement was evaluated by the Fleiss kappa test (multiple raters).

In assessing the fundus position of the demarcation line, we noted that the angle between the line connecting the foveola and the disc

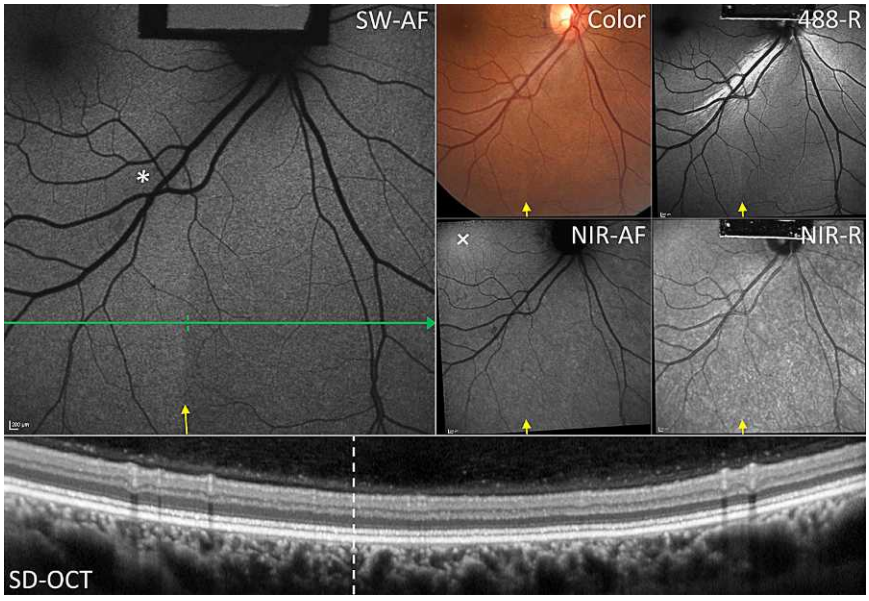

Figure 1. Thirty-degree images of the fundus inferior to the disc from a 42-year-old white female subject (refraction: −1.9 diopters; brown irides). The *rectangle at the top of images* acquired with the Spectralis-SLO is the internal reference used for quantitative assessment of AF. SW-AF: A curved demarcation line is visible inferior to the optic disc. AF on the nasal side of the demarcation line is lower than on the temporal side. This becomes more apparent with increasing distance from the disc. The area where the NFL is thickest correlates with a slight attenuation of AF (*). The *green line* indicates the position of the SD-OCT scan shown below. *Color image*: The boundary is visible at the position of the demarcation line on SW-AF (*yellow arrow*). On the nasal side of the boundary, the choroidal vasculature is more visible and the fundus appears to have a more reddish color. 488-R: The boundary is visible with reduced contrast at the same location as on SW-AF. NIR-AF: The boundary is not visible, but the contribution of RPE melanin at this eccentricity is small compared to that at the fovea, where RPE NIR-AF dominates (*cross*). Subtle changes in RPE melanin AF are overwhelmed by the strong AF from choroidal melanin. NIR-R: No boundary is detected at the site of the demarcation line on SW-AF (*yellow arrow*), probably because—as is the case for NIR-AF—of the overwhelming signal from the deeper layers. SD-OCT: Horizontal 9-mm SD-OCT scan across the inferonasal region at the site indicated by the *green line*; the *interrupted line* indicates the position of the demarcation line on SW-AF. No abrupt changes in retinal structure are visible. The choroid is thinner nasal to the demarcation, but the transition from thick to thin is gradual.

center and a horizontal line was 3.8 ± 3.8° for right eyes, significantly smaller than the 6.5 ± 2.7° for left eyes in this study (Mann-Whitney, $Z = 2.4$, $P = 0.01$) and also smaller than 5.6 to 6.1° observed in larger populations.[10] To minimize for this obvious bias caused by head position during acquisition of the right-eye images, we rotated all right-eye tracings by 2.7° counterclockwise.

Mean gray levels (GL, corrected for the zero-light GL)[2] were measured using Igor software (WaveMetrics, Lake Oswego, OR) on both sides of the demarcation at 10, 15, 20, and 25° inferior to the disc center in both SW-AF and 488-R images. The sampling areas were two rectangles (100 × 25 pixels; separation: 50 pixels) that were positioned on both sides of the demarcation line (necessitating rotation of the image in some cases). The ratios of the mean GL nasal to the line to those temporal to the line were calculated at each position (the ratio was set to 1 if the demarcation was not visible). The ratios of left and right eyes of the same subject were averaged. Data evaluations were done using nonparametric statistics.

All procedures adhered to the tenets of the Declaration of Helsinki, and written informed consent was obtained from all subjects after a full explanation of the procedures was provided. The protocol was approved by the Institutional Review Board of Columbia University.

Results

A curved demarcation line visible with varying degrees of contrast on SW-AF inferior to the optic disc was observed in 31 out of 32 subjects (Figs. 1, 2). The open side of the curved demarcation line was always directed toward the nasal side.

The fundus location of the demarcation line was similar for all eyes (Fig. 3). Accuracy of this data was somewhat compromised by the fact that we did not monitor for head tilt during imaging (see Methods). The locations of the line between eyes of the same subject were symmetrical, although the shape of the line varied slightly; at 20° below the center of the disc the line was within ±2° horizontally (after vertically turning the images of left eyes and aligning the lines between the fovea and the disc center). The line could not be detected at distances shorter than 10° from the disc center, as its course was often masked by large vessels and by nerve fibers converging near the disc. For distances larger than 25° from the disc center, the line could be traced in 55° SW-AF images to approximately 35° inferiorly (data not shown). The position of the demarcation was always nasal to the radial area of thickest nerve fiber layer (NFL) as judged by a slight darkening in the SW-AF images (Fig. 1; asterisk).

For the subgroup of 12 eyes that had other types of imaging, the demarcation line that was seen on SW-AF images in all eyes was observed at the same retinal location by the three observers for 10/12 eyes on 488-R images and for 6/12 eyes on color images. Interobserver agreement was substantial for 488-R images (kappa = 0.77, $P < 0.0001$) and moderate for the color images (kappa = 0.52, $P = 0.0009$).[11] The demarcation line was never detected on NIR-R or on NIR-AF images. In SD-OCT images, there were no apparent features that differentiated structures at or on either side of the demarcating line seen on SW-AF. The choroid on the nasal side was thinner, but the transition was more gradual, occurring over approximately 5 to 15°.

The nasal-temporal ratio of AF relative to the demarcation line was between 0.75 (highest contrast) and 1.0 (line not visible), the median ratios decreasing with increasing distance from the disc center (Fig. 4). The ratios at 15, 20, and 25° from the disc center correlated significantly with each other (Spearman rho >= 0.36, $P < 0.04$). The mean ratios for those

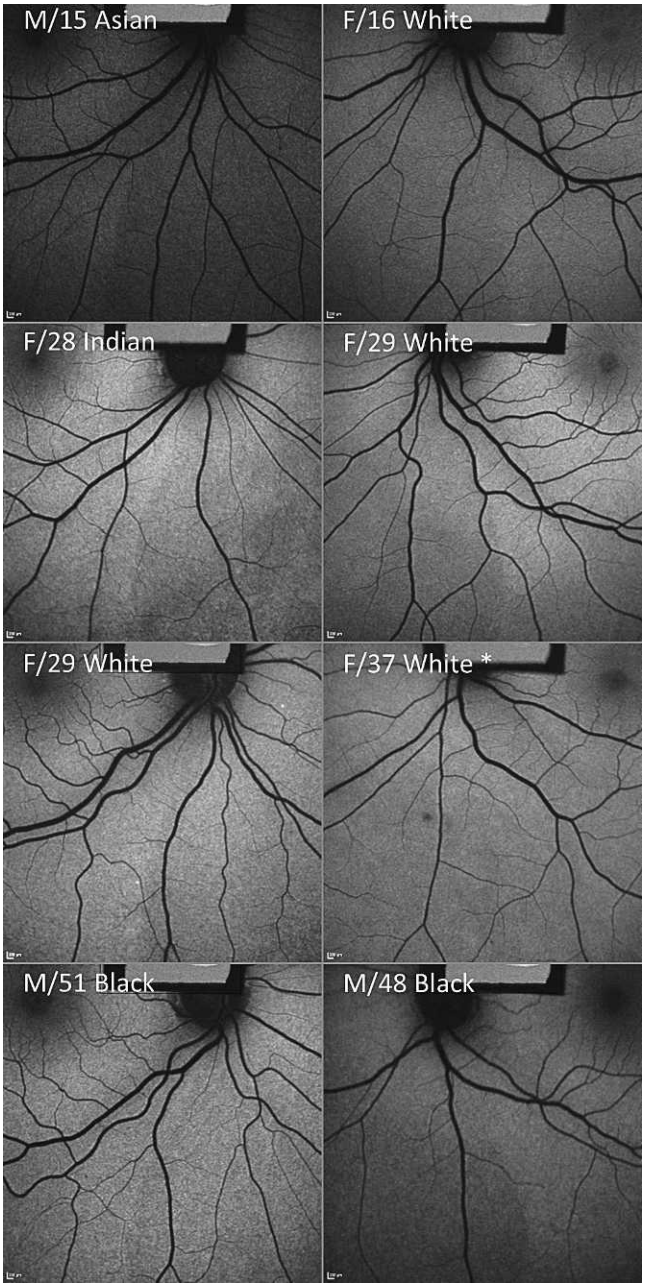

Figure 2. Representative examples of the demarcation line seen in 30° SW-AF images of the region inferior to the optic disc. Sex/age and race as indicated for each image. The demarcation line is visible in most examples as the boundary between low AF nasally and higher AF temporally. Subject F/37 (*), a white female with blue irides and a refraction of −9 diopters, was the only subject from the study group for whom no demarcation line was clearly visible on SW-AF.

three locations were not significantly different for left and right eyes of the same subject (Wilcoxon paired test, $Z = 0.6$, $P = 0.5$) but correlated significantly with each other (Spearman rho $= 0.67$, $P = 0.003$). The ratios (averaged between eyes when both eyes were tested) were not significantly correlated with age (Spearman rho $= 0.13$, $P = 0.4$) and refractive error (Spearman rho $= -0.2$, $P = 0.2$). No significant differences were found between sexes (Mann-Whitney, $Z = 0.30$, $P = 0.7$), between whites and nonwhites ($Z = 0.9$, $P = 0.3$), or between whites with brown and blue iris ($Z = 0.7$, $P = 0.4$).

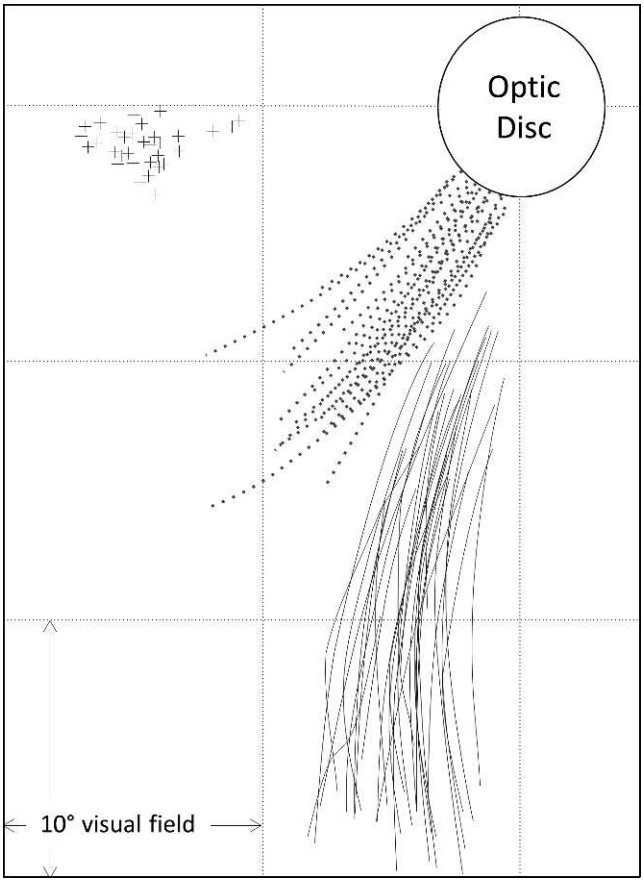

Figure 3. Fundus location of the demarcation line in all subjects ($n = 31$) identified by tracings of that line and referenced to the location of the center of the optic disc. The grid is $10 \times 10°$ of visual field. Tracings from left eyes were turned vertically. Also shown is the position of the foveolas (*crosses*) and the location of the thickest NFL (*dotted line*) as traced from a subtle darkening in the SW-AF image (only seen in 22 subjects).

The median nasal-temporal ratio at the three locations for the initial group, 0.87 (interquartile range [IQR] = 0.04), was significantly lower than that for all other images, 0.91 (IQR = 0.05) ($Z = 2.2$, $P = 0.02$). Thus, the higher contrast of the demarcation line observed for this initial group may reflect the selection process used for that group. However, this did not affect the above statistical outcomes in regard to the correlation between eyes and correlations with age, sex, refraction, and iris color.

For the subgroup of 12 subjects, the nasal-temporal ratio of 488-R was significantly higher (lower contrast) than the SW-AF ratio at the same location (Wilcoxon paired test, $Z > 2.5$, $P < 0.009$ at 15 and 20° and $Z = 1.7$, $P = 0.08$ at 25°). The nasal-to-temporal ratio of 488-R correlated with the ratio of SW-AF when only the nine subjects with dark irides were considered (minimizing choroidal contributions, Spearman rho $= 0.78$, $P = 0.01$), but not for all 12 subjects (Spearman rho $= 0.39$, $P = 0.2$).

Discussion

A distinct demarcation line was seen inferior to the optic disc in the majority of SW-AF images of normal subjects that we studied. This curved line serves as the boundary between two retinal areas of different AF intensities, with up to 25% lower

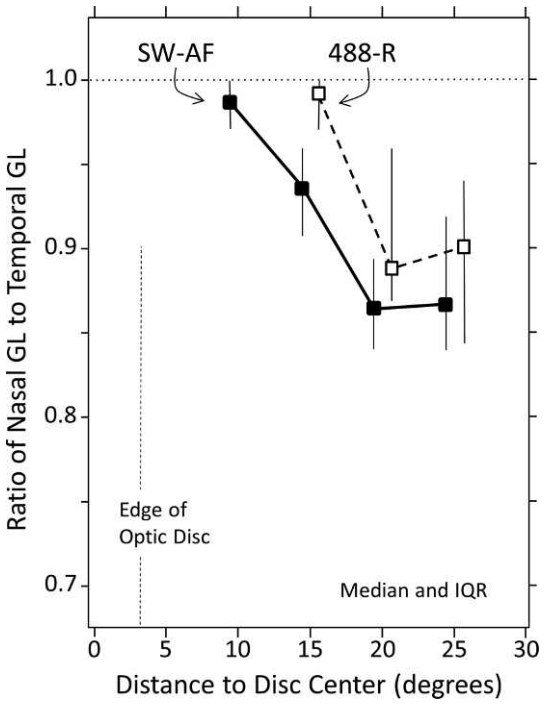

Figure 4. Median ratios of the GL nasal to the line to that temporal to the line for SW-AF images (32 subjects, *solid square, thick line*) and for 488-nm reflectance images (12 subjects, *open squares, dashed line*) as a function of the vertical distance to the disc center. *Brackets* represent the IQR.

levels on the nasal side. This boundary is also seen with reduced clarity in approximately 80% of the 488-R and 50% of color images, but not in NIR-R and NIR-AF images. The abrupt AF change across the demarcation line and the consistently lower AF levels on the nasal relative to the temporal side may be indicative of distinct structural (anatomical) differences between the two regions. The location of the demarcation line inferior to the optic disc may indicate a relationship to the closed optic fissure. The latter forms during the embryological development of the eye through linear invaginations along the inferior surface of the optic stalk and the optic vesicle. This cleft enables the exiting of ganglion cell axons and entrance of the hyaloid artery. Between the fifth and sixth week of gestation, the margins of the fissure approach each other and fuse.[12] Incomplete closure can result in a coloboma, which is typically located inferior to the optic nerve.[13]

The distinctness of the demarcation line signifies that the difference in AF originates in the RPE, the only layer that contributes substantially to the SW-AF.[1] Accordingly, this transition is not a result of modulation of the AF excitation or emission light by either absorption or scattering in the anterior layers. For instance, light scattering by the NFL causes a slight attenuation of the AF in areas of the fundus where the NFL is thickest (Fig. 1; asterisk). However, such attenuation could not account for the demarcation because the thickest NFL is always located temporal and not nasal to the boundary (Fig. 3) and because no abrupt NFL thickness change was detected in birefringence and morphometric studies of NFL thickness.[14,15] Moreover, the concavity of the SW-AF demarcation always faces nasally (Fig. 3), whereas the nerve fiber striations form an arch with the concavity facing the temporal side. Photoreceptor cell absorption could not account for the border, since the photopigments were bleached in our imaging protocol.

It is also unlikely that optical effects in the deeper layers can account for the demarcation line seen in SW-AF. AF emitted from the RPE toward the deeper layers is efficiently reflected back by the choroid for wavelengths longer than 580 nm (reflectance is 7–20%).[16] This would contribute to the demarcation only if the amount of choroidal melanin varied suddenly in the area of the line. However, such variation is not seen in NIR-AF images (Fig. 1), which allow for visualization of melanin in the choroid and RPE.[5] Furthermore, SD-OCT imaging indicated that the choroid was thinner, and thus less pigmented, nasal to the line, confirming other studies.[17–19] The transition between thicker and thinner choroid extends over a distance of 5 to 15° and cannot therefore account for the distinct demarcation.

In addition to reduced SW-AF on the nasal side of the demarcation, we also observed reduced 488-R in that area, with a distinct, albeit less contrasting, boundary (Figs. 1, 4). At that wavelength, light transmitted by the RPE is strongly absorbed in the choroid (particularly in darkly pigmented subjects) such that the predominant fundus reflector of blue-green light is the RPE.[20,21] Since this reflection is thought to be caused by multiple scattering by RPE melanin granules,[22] the diminished reflectance on the nasal side of the demarcation could result from reduced numbers of melanin granules per unit area of retina. This lower melanin content of the RPE may also be responsible, in color fundus images, for the enhanced visibility of choroidal vessels and the slightly brighter, more reddish fundus appearance nasal to the boundary (Fig. 1). Indeed, fewer melanin granules per unit area nasal to the boundary would increase the light transmission to the choroid and reduce RPE reflection by scattering and thus lead to less veiling of choroidal details. Nerve fibers in the area of the demarcating line in the inferior retina are less well visualized than superiorly, both in color and in red-free photography, because of the brighter and uneven choroidal reflection inferiorly.[23]

The lower amount of RPE melanin on the nasal side of the boundary cannot explain the lower SW-AF since reduced absorption of the excitation and emitted AF by RPE melanin would increase the AF nasal to the line, which is not consistent with our observation. This also means that the ratio of nasal to temporal SW-AF would be decreased (more contrast) if the influence of RPE melanin absorption were taken into account. Thus, the actual difference in lipofuscin per unit area may be more pronounced than is implied by the measurements.

While the location of the demarcation line suggests a relationship to the position of optic fissure closure, an explanation for the reduction in RPE melanin and lipofuscin per unit area across the boundary is not obvious. As discussed above, indirect optical effects cannot account for the demarcation line. Nevertheless, differences in melanin and lipofuscin per unit area could occur if the RPE cells on the nasal side of the demarcation were shorter and wider and those temporal to it were taller and narrower, with the same melanin and lipofuscin content of RPE cells in both regions. RPE cell density decreases, and cell width increases, gradually with increasing eccentricity from the fovea. At 50 to 60°, the cell density is half of the central density.[24,25] However, little is known about RPE shape and pigment content in the area inferior to the disc. No difference in the height of RPE cells across the demarcation line could be visualized on OCT. Nevertheless, this possibility cannot be excluded since the optical axial depth resolution of the Spectralis SD-OCT is currently only approximately 7 μm. The correlation of the nasal-temporal ratio in SW-AF with that measured in 488-R also supports a common mechanism, such as a change in RPE cell shape (both height and width) across the boundary. Nonethe-

less, we cannot exclude other factors such as a difference in RPE multinucleation.[26]

Limitations of the study included the mixed study design between the initial exploratory group of subjects used for multimode imaging and the subsequent group, which, coupled with the small number of study subjects, did not give us an exact estimate of the magnitude of the AF discontinuity and its variability in the general population. In addition, histological studies were not performed, and the resolution of OCT is not sufficient to provide an anatomical basis for our findings.

In summary, we observed a curved demarcation line inferior to the optic disc in SW-AF fundus images from healthy subjects. AF levels on the nasal side of the line are lower than on the temporal side. These findings are visible in most subjects and may therefore reflect a normal structural difference between two areas in the inferonasal quadrant. The location of the demarcation line suggests a relationship to the closed optic fissure. We cannot provide a definitive explanation for the observed difference in AF, but the possibilities that have been discussed may warrant further investigation.

Acknowledgments

The authors thank Russell Woods from Harvard University and Carol Mason from Columbia University for their helpful comments and discussions.

References

1. Delori FC, Dorey CK, Staurenghi G, Arend O, Goger DG, Weiter JJ. In vivo fluorescence of the ocular fundus exhibits retinal pigment epithelium lipofuscin characteristics. *Invest Ophthalmol Vis Sci*. 1995;36:718–729.
2. Delori F, Greenberg JP, Woods RL, et al. Quantitative measurements of autofluorescence with the scanning laser ophthalmoscope. *Invest Ophthalmol Vis Sci*. 2011;52:9379–9390.
3. Spaide RF, Klancnik JM Jr. Fundus autofluorescence and central serous chorioretinopathy. *Ophthalmology*. 2005;112:825–833.
4. Schmitz-Valckenberg S, Fleckenstein M, Scholl HP, Holz FG. Fundus autofluorescence and progression of age-related macular degeneration. *Surv Ophthalmol*. 2009;54:96–117.
5. Keilhauer CN, Delori FC. Near-infrared autofluorescence imaging of the fundus: visualization of ocular melanin. *Invest Ophthalmol Vis Sci*. 2006;47:3556–3564.
6. Gomes NL, Greenstein VC, Carlson JN, et al. A comparison of fundus autofluorescence and retinal structure in patients with Stargardt disease. *Invest Ophthalmol Vis Sci*. 2009;50:3953–3959.
7. Heussen FM, Vasconcelos-Santos DV, Pappuru RR, Walsh AC, Rao NA, Sadda SR. Ultra-wide-field green-light (532-nm) autofluorescence imaging in chronic Vogt-Koyanagi-Harada disease. *Ophthalmic Surg Lasers Imaging*. 2011;42:272–277.
8. Slotnick S, Sherman J. Panoramic autofluorescence: highlighting retinal pathology. *Optom Vis Sci*. 2012;89:E575–584.
9. Witmer MT, Kozbial A, Daniel S, Kiss S. Peripheral autofluorescence findings in age-related macular degeneration. *Acta Ophthalmol*. 2012;90:e428–e433.
10. Rohrschneider K. Determination of the location of the fovea on the fundus. *Invest Ophthalmol Vis Sci*. 2004;45:3257–3258.
11. Landis JR, Koch GG. The measurement of observer agreement for categorical data. *Biometrics*. 1977;33:159–174.
12. Geeraets R. An electron microscopic study of the closure of the optic fissure in the golden hamster. *Am J Anat*. 1976;145:411–431.
13. Onwochei BC, Simon JW, Bateman JB, Couture KC, Mir E. Ocular colobomata. *Surv Ophthalmol*. 2000;45:175–194.
14. Cense B, Chen TC, Park BH, Pierce MC, de Boer JF. Thickness and birefringence of healthy retinal nerve fiber layer tissue measured with polarization-sensitive optical coherence tomography. *Invest Ophthalmol Vis Sci*. 2004;45:2606–2612.
15. Cohen MJ, Kaliner E, Frenkel S, Kogan M, Miron H, Blumenthal EZ. Morphometric analysis of human peripapillary retinal nerve fiber layer thickness. *Invest Ophthalmol Vis Sci*. 2008;49:941–944.
16. Delori FC. Spectrophotometer for noninvasive measurement of intrinsic fluorescence and reflectance of the ocular fundus. *Appl Opt*. 1994;33:7439–7452.
17. Ikuno Y, Kawaguchi K, Nouchi T, Yasuno Y. Choroidal thickness in healthy Japanese subjects. *Invest Ophthalmol Vis Sci*. 2010;51:2173–2176.
18. Ouyang Y, Heussen FM, Mokwa N, et al. Spatial distribution of posterior pole choroidal thickness by spectral domain optical coherence tomography. *Invest Ophthalmol Vis Sci*. 2011;52:7019–7026.
19. Tanabe H, Ito Y, Terasaki H. Choroid is thinner in inferior region of optic disks of normal eyes. *Retina*. 2012;32:134–139.
20. Delori FC, Pflibsen KP. Spectral reflectance of the human ocular fundus. *Appl Opt*. 1989;28:1061–1077.
21. van de Kraats J, Berendschot TT, van Norren D. The pathways of light measured in fundus reflectometry. *Vis Res*. 1996;36:2229–2247.
22. Sardar DK, Mayo ML, Glickman RD. Optical characterization of melanin. *J Biomed Opt*. 2001;6:404–411.
23. Quigley HA. *Diagnosing Early Glaucoma with Nerve Fiber Layer Examination*. Baltimore, MD: Williams & Wilkins; 1995.
24. Panda-Jonas S, Jonas JB, Jakobczyk-Zmija M. Retinal pigment epithelial cell count, distribution, and correlations in normal human eyes. *Am J Ophthalmol*. 1996;121:181–189.
25. Harman AM, Fleming PA, Hoskins RV, Moore SR. Development and aging of cell topography in the human retinal pigment epithelium. *Invest Ophthalmol Vis Sci*. 1997;38:2016–2026.
26. Fleming PA, Harman AM, Beazley LD. Changing topography of the RPE resulting from experimentally induced rapid eye growth. *Vis Neurosci*. 1997;14:449–461.